

Reference ranges for fetal venous and atrioventricular blood flow parameters

K. Hecher, S. Campbell, R. Snijders and K. Nicolaides

Department of Obstetrics and Gynaecology and Harris Birthright Research Centre for Fetal Medicine, King's College Hospital Medical School, London, UK

Key words: DOPPLER ULTRASOUND, FETAL CIRCULATION, FETAL VENOUS FLOW, FETAL CARDIAC FLOW, DUCTUS VENOSUS

ABSTRACT

This cross-sectional study establishes reference ranges with gestation for Doppler parameters of fetal venous and atrioventricular blood flow. Color flow Doppler was used to examine 143 normal singleton pregnancies at 20–40 weeks' gestation. Flow velocity waveforms were recorded from the ductus venosus, right hepatic vein and inferior vena cava. The waveforms are triphasic, reflecting ventricular systole, early diastole and atrial contraction. Peak velocities for these parameters were measured with pulsed Doppler and a new index, the peak velocity index for veins (PVIV), was calculated. Similarly, time-averaged maximum velocities for the whole cardiac cycle were measured and the pulsatility index for veins (PIV) was calculated. Flow velocity waveforms were also recorded at the level of the atrioventricular valves and the ratios of peak velocities at early diastolic filling (E) and atrial contraction (A) were calculated. Regression analysis was used to define the association of each measured and calculated Doppler parameter with gestational age. Blood flow velocities in the fetal veins and velocities and E/A ratios across the atrioventricular valves increased significantly with gestation, whereas PVIV and PIV decreased. Blood flow velocities were highest in the ductus venosus and lowest in the right hepatic vein, and PVIV and PIV were highest in the hepatic vein and lowest in the ductus venosus. In the ductus venosus, there was always forward flow throughout the heart cycle, whereas in the inferior vena cava and hepatic vein during atrial contraction, flow was away from or towards the heart or there was no flow. Pulsatility of flow velocity waveforms in the venous system is the consequence of changes in pressure difference between the venous system and the heart during the heart cycle. The finding that PVIV and PIV decrease with gestation is consistent with decreasing cardiac afterload and maturation of diastolic ventricular function.

INTRODUCTION

Color flow imaging and Doppler velocimetry have made it possible to examine fetal venous and intracardiac blood

flow. Several studies have examined individual vessels and reported differences between normal and pathological pregnancies. The aim of this study was to establish reference ranges with gestation for blood flow velocities and indices of pulsatility for flow in the ductus venosus, inferior vena cava, right hepatic vein and atrioventricular valves.

PATIENTS AND METHODS

This was a cross-sectional study of 143 women with singleton pregnancies at 20–40 weeks' gestation who were recruited consecutively from our routine antenatal clinic or fetal assessment center and agreed to participate in this study. Entry criteria were as follows: gestation was calculated from the menstrual history and confirmed by fetal biometry at 20 weeks' amenorrhea. In all cases the fetuses were found to be anatomically normal at the time of the ultrasound examination and this was subsequently confirmed at delivery. In addition, fetal head and abdominal circumferences were within the 90% confidence interval of our normal ranges and fetal movements, amniotic fluid volume and pulsatility index of the umbilical artery and middle cerebral artery were also normal.

Pulsed wave Doppler ultrasound studies of the fetal circulation were performed with a color Doppler system (Acuson 128, Mountain View, California) with a 3.5-MHz or 5-MHz curved array transducer with spatial peak temporal average intensities below 100 mW/cm². The high-pass filter was set at 125 Hz. The size of the sample volume was adapted to the vessel diameter in order to cover it entirely. All recordings used for measurements were obtained in the absence of fetal breathing movements and the angle between the ultrasound beam and the direction of blood flow was less than 50° for venous vessels and less than 30° for recordings at atrioventricular valve level. The fetal heart rate was within the normal range of 120–160 beats/min.

Flow velocity waveforms were recorded from the ductus venosus, the right hepatic vein and the inferior

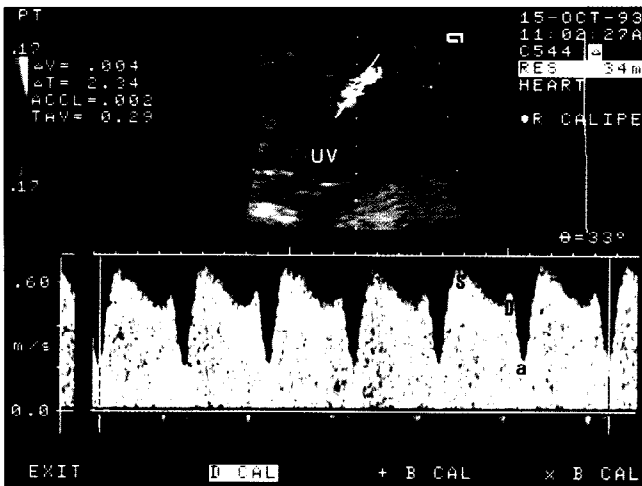


Figure 1 Visualization of the ductus venosus in a longitudinal plane. The umbilical vein (UV) runs cephalad in a convex curvature and the ductus venosus arises in a concave curvature towards the heart. The sample volume was positioned immediately at the inlet of the ductus venosus, where color Doppler indicated a marked increase of velocities. Blood flow velocity waveforms showed that there was blood flow towards the heart throughout the heart cycle. *S*, peak systolic velocity; *D*, peak diastolic velocity; *a*, atrial contraction

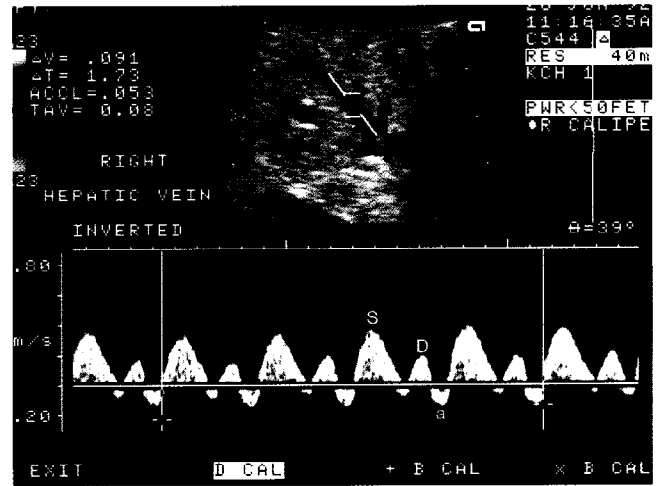


Figure 2 Visualization of the right hepatic vein in an oblique transverse plane through the upper abdomen. The sample volume was positioned in the main stem of the vessel distal to the subdiaphragmatic venous confluence and proximal to the division into its branches. Blood flow velocity waveforms showed a marked reverse flow component during atrial contraction (*a*), and there was little reverse flow between the systolic (*S*) and diastolic (*D*) peaks, which can be seen in a minority of cases

vena cava. The ductus venosus was visualized either in a mid-sagittal longitudinal plane of the fetal trunk or in an oblique transverse plane through the upper abdomen. The sample volume was positioned at its origin from the umbilical vein, where color Doppler indicated the highest velocities (Figure 1). The right hepatic vein was depicted either in an oblique transverse plane more cephalic than the one for the umbilical vein or in a sagittal-coronal view of the right lobe of the liver, and the sample volume was positioned in the main stem of the vessel (Figure 2). Flow velocity waveforms from the inferior vena cava were recorded in a longitudinal section with the sample volume placed in the portion between the renal and the hepatic veins (Figure 3).

After angle correction, the following parameters were measured as mean values of at least three consecutive uniform waveforms (Figures 1–3):

- (1) Peak forward velocity during ventricular systole (*S*);
- (2) Peak forward velocity during early diastole (*D*) which corresponds to passive ventricular filling;
- (3) Lowest forward velocity or peak reversed velocity during atrial contraction (*a*) in late diastole;
- (4) Time-averaged maximum velocity (*Tamx*) by following the maximum frequency envelope of the flow velocity waveform of one heart cycle;
- (5) Intensity-weighted time-averaged mean velocity (V_m); and
- (6) Fetal heart rate.

Two indices for venous waveforms which are independent of the angle of insonation were calculated. The first, peak velocity index for veins (PVIV) was defined

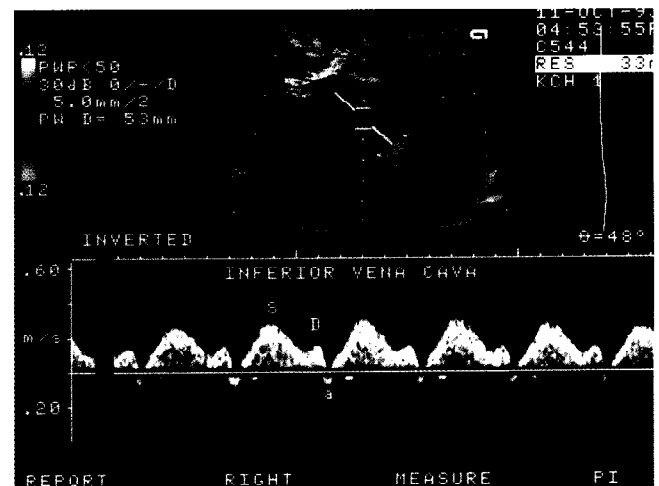


Figure 3 Visualization of the inferior vena cava in a longitudinal plane. The sample plane was positioned between confluence of the hepatic veins and the renal vein. The renal vessels are depicted in the top left-hand corner. Blood flow velocity waveforms showed only a little reverse component with atrial contraction (*a*), compared to the forward component throughout systole (*S*) and early diastole (*D*)

as $(S - a)/D$, and the second, pulsatility index for veins (PIV), was defined as $(S - a)/Tamx$. The PIV is practically the same as the PI for arterial vessels, allowing for reverse flow during diastole¹.

Tricuspid and mitral ventricular inflow velocity waveforms were recorded from a four-chamber view of the fetal heart and the sample volume was placed immediately below the level of the valves in the right and left ventricle, respectively (Figure 4). Peak flow velocities in early diastole (*E*) and late diastole with atrial contraction (*A*) were measured and the *E/A* ratio was calculated as a mean value of three heart cycles.

Statistical analysis

For each of the Doppler parameters and their indices, regression analysis was applied to derive formulas for the

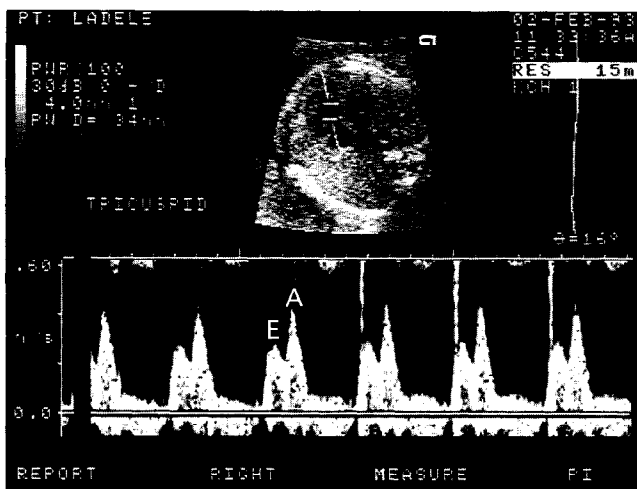


Figure 4 Doppler waveform of the ventricular inflow through the tricuspid valve. The sample volume was positioned in the right ventricle immediately below the plane of the valve. *E*, peak velocity with rapid filling during early diastole; *A*, peak velocity with atrial contraction

association with gestational age. For those measurements where the standard deviation increased or decreased with gestation, logarithmic transformation was applied to stabilize variance. The regression lines on transformed data were used to calculate the mean and residual SD in transformed units. To produce the reference ranges in original units the limits of the calculated reference range were subjected to anti-logarithmic transformation². The correlation of Doppler parameters with fetal heart rate was investigated.

RESULTS

The percentage distribution of ethnic origin of the women was Caucasian (47%), Afro-Caribbean (43%) and Asian (10%). In 32 cases (22%) the mothers were cigarette smokers. The mean gestational age at delivery was 278 days (SD = 11), and the mean birth weight was 3250 g (SD = 455). The percentage of neonates with a birth weight below the fifth centile corrected for gestational age and sex³, and the Cesarean section rate were 4.9% and 14.6%, respectively. The mean birth weight of the overall population of the hospital during the study period was 3230 g and the Cesarean section rate was 16.3%.

Table 1 Regression equations for various Doppler measurements and their ratios with gestational age (GA). For those parameters where the standard deviation (SD) increased or decreased with gestation, logarithmic transformation was applied to stabilize variance. *A*, coefficient for linear component; *B*, coefficient for quadratic component

Parameter	Transformation	Constant	$A \times GA$	$B \times GA^2$	SD
<i>Inferior vena cava</i>					
V_m	log ₁₀	0.480	0.0189	—	0.0926
Tamx	—	-0.807	0.7352	—	4.8000
Systolic peak (<i>S</i>)	—	10.463	0.8474	—	8.1157
Diastolic peak (<i>D</i>)	log ₁₀	0.930	0.0129	—	0.1040
<i>a</i> wave	—	-28.086	1.0510	—	7.2853
(<i>S</i> - <i>a</i>)/ <i>D</i>	log ₁₀	0.623	-0.0149	—	0.1554
(<i>S</i> - <i>a</i>)/Tamx	log ₁₀	0.722	-0.0178	—	0.1490
<i>Ductus venosus</i>					
V_m	—	16.216	0.5820	—	5.7470
Tamx	—	-21.174	5.4000	-0.082	10.004
Systolic peak (<i>S</i>)	—	-27.589	6.7890	-0.106	11.295
Diastolic peak (<i>D</i>)	—	-18.718	5.6560	-0.088	10.802
<i>a</i> wave	—	-29.855	4.0260	-0.052	9.4656
(<i>S</i> - <i>a</i>)/ <i>D</i>	—	0.805	-0.0099	—	0.1239
(<i>S</i> - <i>a</i>)/Tamx	—	0.903	-0.0116	—	0.1483
<i>Right hepatic vein</i>					
V_m	log ₁₀	0.421	0.0134	—	0.1231
Tamx	—	4.729	0.2615	—	3.0494
Systolic peak (<i>S</i>)	—	14.451	0.4450	—	5.4670
Diastolic peak (<i>D</i>)	—	14.827	—	—	3.9070
<i>a</i> wave	—	-18.881	0.3554	—	4.1221
(<i>S</i> - <i>a</i>)/ <i>D</i>	—	2.435	—	—	0.4969
(<i>S</i> - <i>a</i>)/Tamx	—	4.753	-0.0587	—	0.6806
<i>Mitral valve</i>					
<i>E</i> wave	—	21.034	0.5080	—	5.5830
<i>A</i> wave	—	52.109	—	—	8.3670
<i>E/A</i>	log ₁₀	-0.369	0.0070	—	0.0488
<i>Tricuspid valve</i>					
<i>E</i> wave	—	18.404	0.8030	—	6.1860
<i>A</i> wave	—	47.204	0.4060	—	8.3620
<i>E/A</i>	—	0.428	0.0098	—	0.0687

Table 2 Correlations with gestational age and fetal heart rate for various Doppler parameters

Parameter	Gestational age	Fetal heart rate
<i>Inferior vena cava</i>		
V_m	0.770*	-0.248 [†]
Tamx	0.679*	-0.132
Systolic peak (S)	0.533*	-0.052
Diastolic peak (D)	0.599*	-0.345*
a wave	0.651*	-0.238
(S - a)/D	-0.501*	0.301 [†]
(S - a)/Tamx	-0.586*	0.162
<i>Ductus venosus</i>		
V_m	0.523*	-0.223
Tamx	0.381 [†]	-0.041
Systolic peak (S)	0.377 [†]	-0.044
Diastolic peak (D)	0.342 [†]	-0.137
a wave	0.535*	-0.096
(S - a)/D	-0.436*	0.157
(S - a)/Tamx	-0.432*	0.079
<i>Right hepatic vein</i>		
V_m	0.544*	-0.172
Tamx	0.457*	-0.126
Systolic peak (S)	0.438*	-0.080
Diastolic peak (D)	0.039	-0.252 [†]
a wave	0.459*	-0.044
(S - a)/D	0.114	0.120
(S - a)/Tamx	-0.459*	0.111
<i>Mitral valve</i>		
E wave	0.477*	-0.271 [†]
A wave	-0.035	0.111
E/A	0.650*	-0.415*
<i>Tricuspid valve</i>		
E wave	0.615*	-0.271 [†]
A wave	0.280 [†]	0.016
E/A	0.652*	-0.339*

*, $p < 0.001$; [†], $p < 0.01$

Clear and uniform Doppler signals were obtained in 94% of cases (134 of 143) from the ductus venosus, in 93% (133 of 143) from the right hepatic vein, and 89% (127 of 143) from the inferior vena cava. It was possible to calculate the E/A ratio in 77% (110 of 143) on the tricuspid side and in 87% (124 of 143) on the mitral side.

Results of the regression analysis for each parameter are given in Table 1 and the reference ranges are shown in Figures 5–31. Table 2 shows the correlation of Doppler parameters with gestational age and fetal heart rate. All velocity measurements increased with gestational age, except for right hepatic vein D velocity and mitral A velocity which did not change significantly with gestation. PVIV and PIV decreased with gestation, except for PVIV in the right hepatic vein which did not change. Both mitral and tricuspid E/A ratios increased with gestation.

Right hepatic vein D velocity and inferior vena cava V_m and D velocity decreased with increasing fetal heart rate. There were no significant changes with fetal heart rate for PVIV and PIV, except for a positive correlation with inferior vena cava PVIV. Both mitral and tricuspid E/A ratios showed significant negative correlations with heart rate, caused by a decrease in E velocities with increasing fetal heart rate.

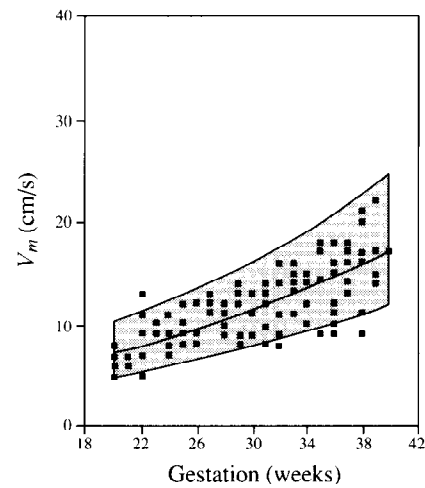


Figure 5 Individual values for the intensity-weighted mean velocity (V_m) in the inferior vena cava of 127 normal fetuses plotted on the appropriate reference range (mean, 5th and 95th centiles) with gestation

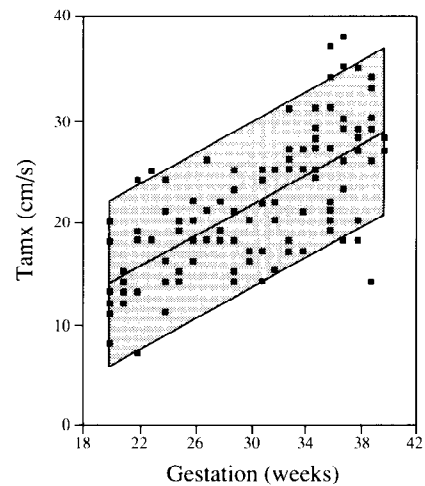


Figure 6 Individual values for the time-averaged maximum velocity (Tamx) in the inferior vena cava of 127 normal fetuses plotted on the appropriate reference range (mean, 5th and 95th centiles) with gestation

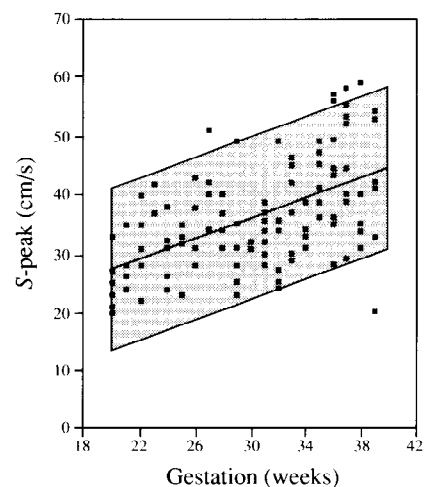


Figure 7 Individual values for the peak systolic velocity (S peak) in the inferior vena cava of 127 normal fetuses plotted on the appropriate reference range (mean, 5th and 95th centiles) with gestation

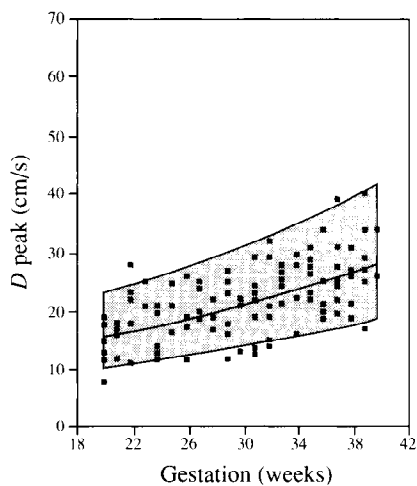


Figure 8 Individual values for the peak diastolic velocity (*D* peak) in the inferior vena cava of 127 normal fetuses plotted on the appropriate reference range (mean, 5th and 95th centiles) with gestation

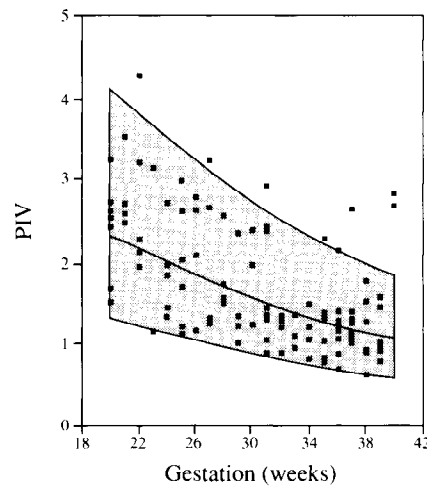


Figure 11 Individual values for PIV ((peak systolic velocity minus lowest velocity during atrial contraction)/time-averaged maximum velocity), in the inferior vena cava of 127 normal fetuses plotted on the appropriate reference range (mean, 5th and 95th centiles) with gestation

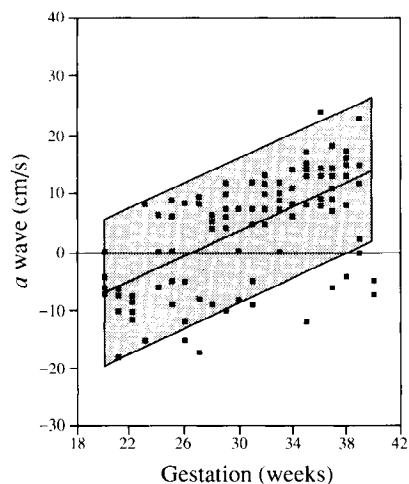


Figure 9 Individual values for the lowest velocity during atrial contraction (*a*) in the inferior vena cava of 127 normal fetuses plotted on the appropriate reference range (mean, 5th and 95th centiles) with gestation

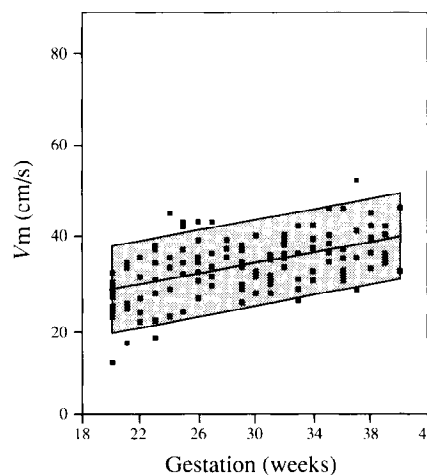


Figure 12 Individual values for the intensity-weighted mean velocity (*V_m*) in the ductus venosus of 134 normal fetuses plotted on the appropriate reference range (mean, 5th and 95th centiles) with gestation

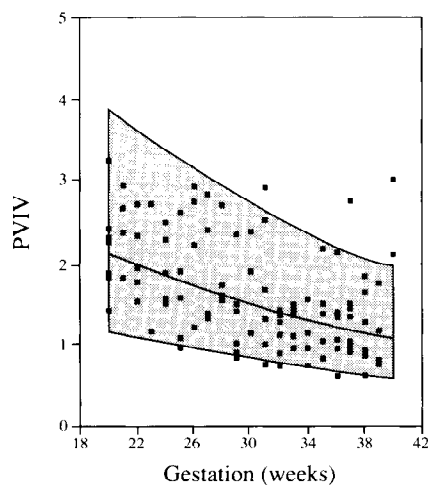


Figure 10 Individual values for PVIV ((peak systolic velocity minus lowest velocity during atrial contraction)/peak diastolic velocity), in the inferior vena cava of 127 normal fetuses plotted on the appropriate reference range (mean, 5th and 95th centiles) with gestation

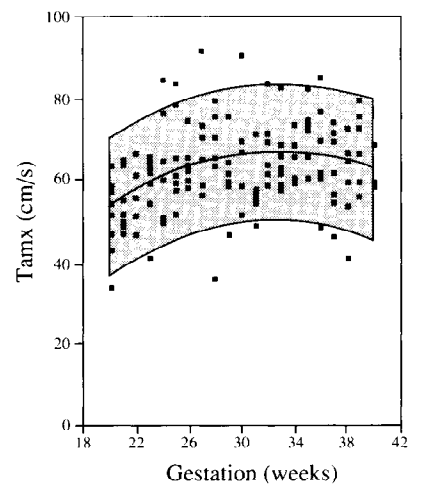


Figure 13 Individual values for the time-averaged maximum velocity (*Tamx*) in the ductus venosus of 134 normal fetuses plotted on the appropriate reference range (mean, 5th and 95th centiles) with gestation

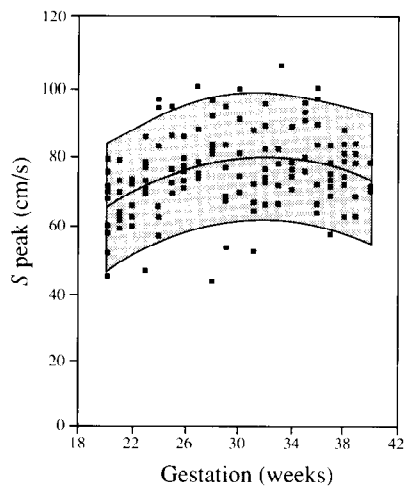


Figure 14 Individual values for the peak systolic velocity (*S* peak) in the ductus venosus of 134 normal fetuses plotted on the appropriate reference range (mean, 5th and 95th centiles) with gestation

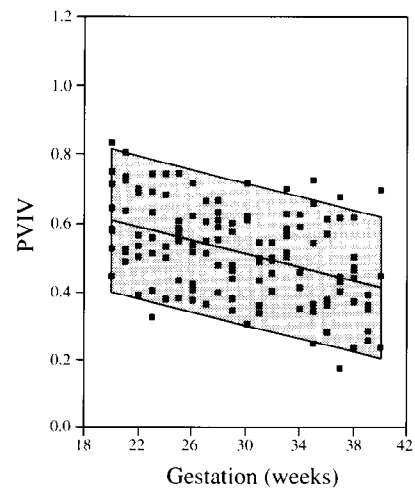


Figure 17 Individual values for the PVIV ((peak systolic velocity minus lowest velocity during atrial contraction)/peak diastolic velocity), in the ductus venosus of 134 normal fetuses plotted on the appropriate reference range (mean, 5th and 95th centiles) with gestation

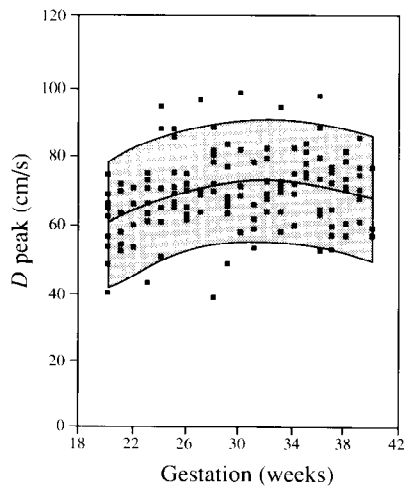


Figure 15 Individual values for the peak diastolic velocity (*D* peak) in the ductus venosus of 134 normal fetuses plotted on the appropriate reference range (mean, 5th and 95th centiles) with gestation

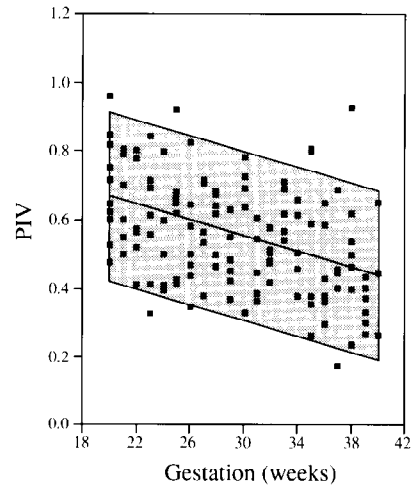


Figure 18 Individual values for the PIV ((peak systolic velocity minus lowest velocity during atrial contraction)/time-averaged maximum velocity), in the ductus venosus of 134 normal fetuses plotted on the appropriate reference range (mean, 5th and 95th centiles) with gestation

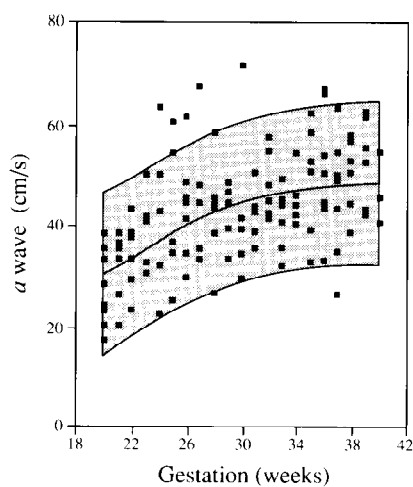


Figure 16 Individual values for the lowest velocity during atrial contraction (*a*) in the ductus venosus of 134 normal fetuses plotted on the appropriate reference range (mean, 5th and 95th centiles) with gestation

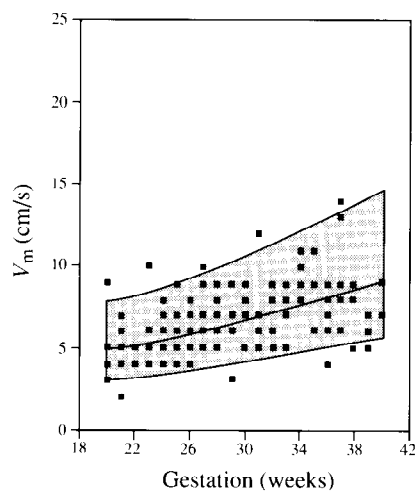


Figure 19 Individual values for the intensity weighted mean velocity (V_m) in the right hepatic vein of 133 normal fetuses plotted on the appropriate reference range (mean, 5th and 95th centiles) with gestation

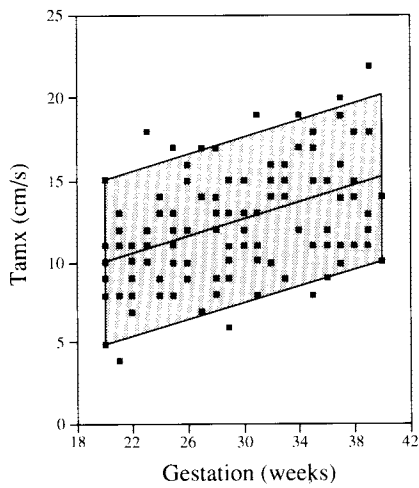


Figure 20 Individual values for the time-averaged maximum velocity (Tamx) in the right hepatic vein of 133 normal fetuses plotted on the appropriate reference range (mean, 5th and 95th centiles) with gestation

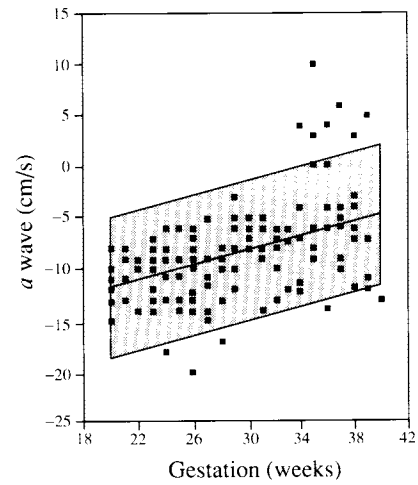


Figure 23 Individual values for the lowest velocity during atrial contraction (*a*) in the right hepatic vein of 133 normal fetuses plotted on the appropriate reference range (mean, 5th and 95th centiles) with gestation

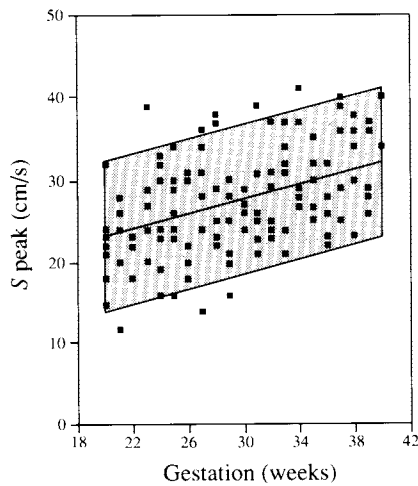


Figure 21 Individual values for the peak systolic velocity (*S* peak) in the right hepatic vein of 133 normal fetuses plotted on the appropriate reference range (mean, 5th and 95th centiles) with gestation

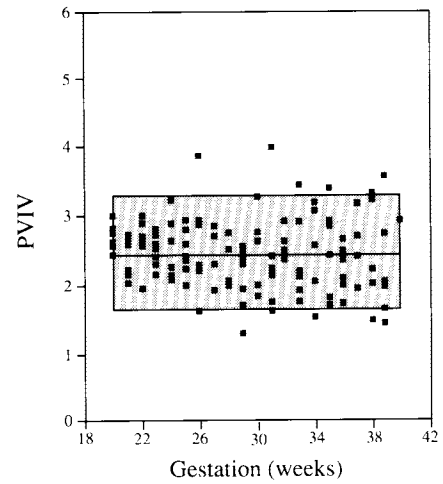


Figure 24 Individual values for PVIV ((peak systolic velocity minus lowest velocity during atrial contraction)/peak diastolic velocity), in the right hepatic vein of 133 normal fetuses plotted on the appropriate reference range (mean, 5th and 95th centiles) with gestation

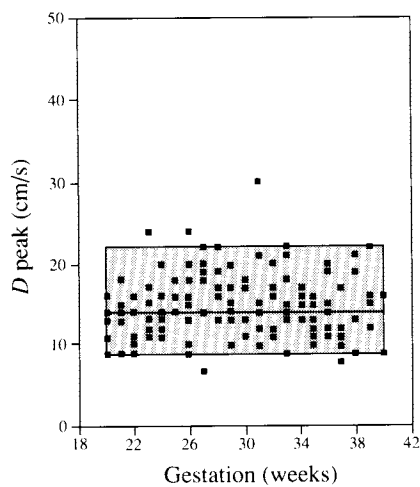


Figure 22 Individual values for the peak diastolic velocity (*D* peak) in the right hepatic vein of 133 normal fetuses plotted on the appropriate reference range (mean, 5th and 95th centiles) with gestation

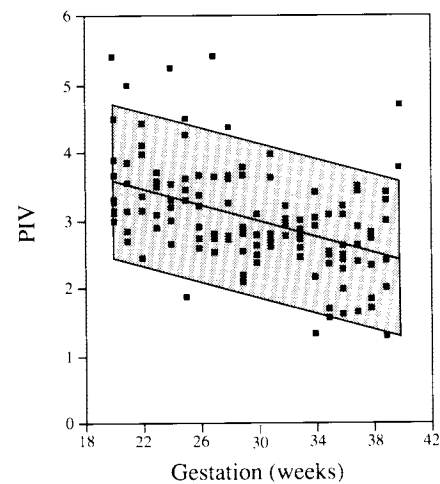


Figure 25 Individual values for PIV ((peak systolic velocity minus lowest velocity during atrial contraction)/time-averaged maximum velocity), in the right hepatic vein of 133 normal fetuses plotted on the appropriate reference range (mean, 5th and 95th centiles) with gestation

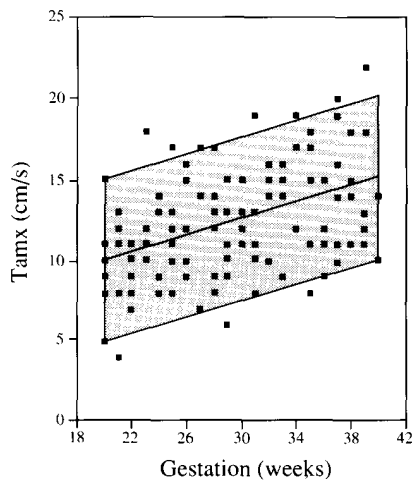


Figure 20 Individual values for the time-averaged maximum velocity (Tamx) in the right hepatic vein of 133 normal fetuses plotted on the appropriate reference range (mean, 5th and 95th centiles) with gestation

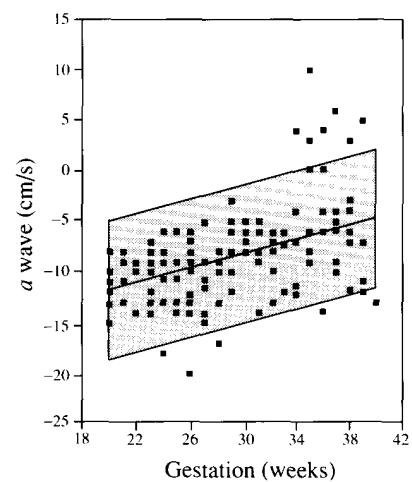


Figure 23 Individual values for the lowest velocity during atrial contraction (*a*) in the right hepatic vein of 133 normal fetuses plotted on the appropriate reference range (mean, 5th and 95th centiles) with gestation

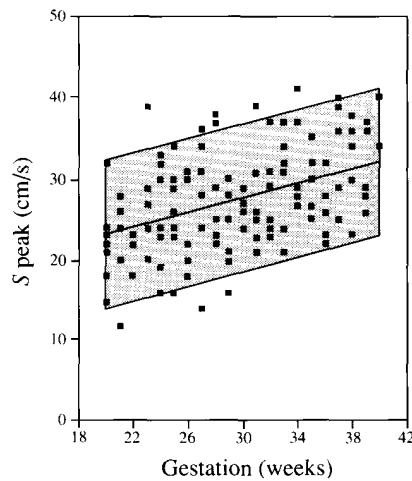


Figure 21 Individual values for the peak systolic velocity (*S* peak) in the right hepatic vein of 133 normal fetuses plotted on the appropriate reference range (mean, 5th and 95th centiles) with gestation

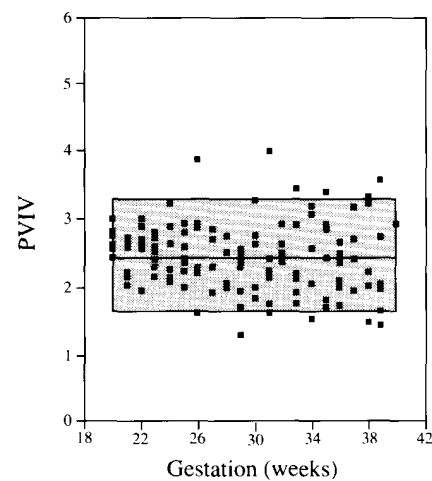


Figure 24 Individual values for PVIV ((peak systolic velocity minus lowest velocity during atrial contraction)/peak diastolic velocity), in the right hepatic vein of 133 normal fetuses plotted on the appropriate reference range (mean, 5th and 95th centiles) with gestation

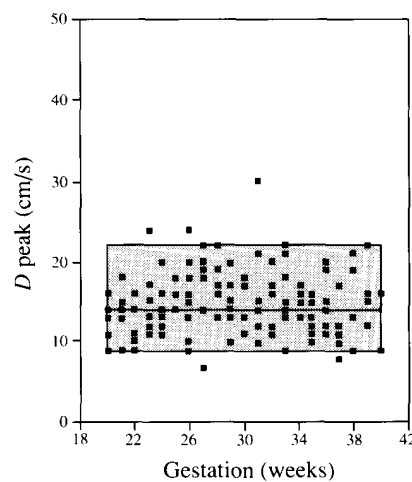


Figure 22 Individual values for the peak diastolic velocity (*D* peak) in the right hepatic vein of 133 normal fetuses plotted on the appropriate reference range (mean, 5th and 95th centiles) with gestation

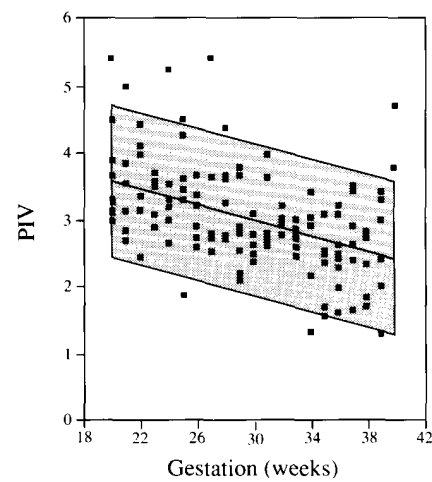


Figure 25 Individual values for PIV ((peak systolic velocity minus lowest velocity during atrial contraction)/time-averaged maximum velocity), in the right hepatic vein of 133 normal fetuses plotted on the appropriate reference range (mean, 5th and 95th centiles) with gestation

DISCUSSION

The data of this study indicate that in venous flow, first, blood velocities increase, whereas PVIV and PIV decrease with advancing gestation; second, velocities are highest in the ductus venosus and lowest in the right hepatic vein, whereas PVIV and PIV are lowest in the ductus venosus and highest in the right hepatic vein; and third, fetal heart rate has no significant influence on the indices within the normal range of 120–160 beats/min. Previous studies on venous flow velocities, which were confined to the ductus venosus, also reported gestation-related increase in velocities^{4,5}. This study has also demonstrated that atrioventricular *E/A* ratios increase with advancing gestation and decrease with increasing fetal heart rate.

During Doppler studies of the fetal circulation, it is essential to avoid measurements during fetal breathing movements. This is well described for the arterial side but it is even more important for venous flow, because the changes in intrathoracic pressure during breathing movements have a profound influence on flow velocity waveforms⁶.

The sampling site also plays an important role in venous Doppler studies. Kiserud and co-workers⁷ reported that velocities at the inlet of the ductus venosus immediately above the umbilical vein are higher than at the outlet into the inferior vena cava; they suggested standardizing the sampling site at the inlet. Huisman and colleagues⁸ recorded inferior vena cava signals at the entrance to the right atrium and found a large standard deviation for various flow velocity waveform parameters. In a subsequent anatomical study, these authors demonstrated a sub-diaphragmatic venous vestibulum, which is the funnel-like end of the inferior vena cava containing also the orifices of the hepatic veins and the ductus venosus⁹. They therefore suggested that, to avoid a mixture of overlapping signals from different blood-streams, flow velocity waveforms from the inferior vena cava and hepatic veins should be obtained more distally. Rizzo and colleagues¹⁰ reported that the highest reproducibility of inferior vena cava flow velocity waveforms is achieved by placing the sample volume between the entrance of the renal vein and the ductus venosus.

In the ductus venosus the direction of blood flow is towards the heart throughout the heart cycle. In the inferior vena cava, during atrial contraction the direction of flow can be away from the heart, zero or toward the heart, and the likelihood of the last increases with gestational age. In the right hepatic vein flow during atrial contraction is generally away from the heart, but in the late third trimester flow can be towards the heart. Venous flow velocity waveforms basically show the same velocity profile in all the investigated vessels; the only difference in waveforms can be produced by a parallel shift of the zero line causing differences in absolute velocities. This can also lead to waveforms where flow during atrial contraction is directed towards and away from the heart at the same time, especially in vessels with relatively low velocities, such as the right hepatic vein.

In these cases velocity during atrial contraction was measured either as lowest forward or peak reversed velocity, depending on which was numerically higher.

The increase in venous flow velocities with gestational age is a logical consequence of the increase of velocities on the arterial side. Arterial output and venous return have to be in balance during gestation. Pulsatility of flow velocity waveforms in the venous system is the consequence of changes in pressure difference between the venous system and the right atrium during the heart cycle. In the case of flow velocity waveforms from the ductus venosus, there is an additional contribution from left atrial pressure during systole and early diastole, when the foramen ovale is open. Kiserud and colleagues¹¹ have demonstrated preferential flow of blood from the ductus venosus through the foramen ovale to the left atrium. However, the foramen ovale is closed during atrial contraction and therefore flow in the ductus venosus flow reflects at that moment the pressure gradient towards the right atrium which itself is dependent on the gradient between the right atrium and ventricle.

The finding that the degree of pulsatility decreases with gestation is consistent with a decrease in cardiac afterload, due to a decrease in placental resistance, which has been shown by numerous studies, and to maturation in diastolic ventricular function. A decrease in cardiac afterload causes a decrease in end-diastolic ventricular pressure and therefore an increase in blood flow velocity during atrial contraction. This seems to be the main reason for a decrease in venous waveform indices with advancing gestation. In particular, in the ductus venosus, flow velocity during atrial contraction shows the most significant increase of all the velocities measured for calculation of indices (Table 2 and Figures 13–16).

Studies attempting to describe the pulsatility of flow velocity waveforms in the inferior vena cava and/or ductus venosus have used the *S/D* ratio, resistance index (*S/a*) or the preload index (*a/S*)^{5,8,12–15}. Both a decrease¹² and no significant change^{8,13} with gestational age have been found in the *S/D* ratio. In both of the last studies there was a significant decrease of percentage of reverse flow with atrial contraction, which the authors explained was the result of an increase in ventricular compliance and a reduction in placental resistance. Recently, DeVore and Horenstein¹⁴ described the ductus venosus index, which is the equivalent to the resistance index and decreases significantly with gestational age. However, these indices do not take into account the triphasic shape of venous blood flow waveforms. The indices we describe give an estimation of the overall pulsatility of the flow velocity waveform: the more pulsatile the flow velocity waveform, the higher the PVIV and PIV. The advantage of using these indices, compared to absolute velocity measurements, is that they are independent of the angle between the Doppler beam and the direction of blood flow. Absolute velocity measurements seem to be error-prone, particularly in the ductus venosus, because of its curvature within a short distance (Figure 1).

The findings of positive correlation between atrioventricular *E/A* ratios and gestational age with a con-

sistently higher *A* than *E* wave and higher velocities on the tricuspid side are compatible with those of previous reports^{16–19}. The finding that the increase in *E/A* ratio with advancing gestation is due to the increase of early diastolic peak *E* velocities indicates that ventricular compliance remains unchanged and that the underlying mechanism is either increased volume flow or improvement of ventricular relaxation^{20,21}. Maturation of fetal cardiac function may also be responsible for the observed changes in venous flow velocity waveforms. The *D* velocity of venous flow velocity waveforms corresponds to the *E* velocity of the flow velocity waveforms from the atrioventricular inflow. Fetal heart rate affects the *E* velocity and this accounts for the negative correlation between heart rate and the *E/A* ratio. This may also be the underlying mechanism for heart rate dependency of *D* velocity in the inferior vena cava and hepatic vein. In some cases the flow velocity waveforms from the tricuspid inflow were monophasic rather than biphasic (*E* and *A* waves), and consequently the number of cases with *E/A* ratios was lower for tricuspid than for mitral inflow. This occurred only in cases where the fetal heart rate was ≥ 140 beats/min. This is in agreement with other authors who reported this finding to be more common with high-normal fetal heart rates¹⁹.

This cross-sectional study establishes reference ranges with gestation for Doppler parameters of fetal venous and cardiac inflow. The population examined was heterogeneous for ethnic background and included cigarette smokers and women whose pregnancies resulted in delivery of small-for-gestational-age infants. However, the percentages of smokers and women with babies with a birth weight below the fifth centile did not exceed those of an average population. The reference ranges can be used for assessment of pregnancies complicated by abnormal fetal cardiac anatomy and pregnancies where a hostile intrauterine environment may alter fetal cardiovascular function.

ACKNOWLEDGEMENT

K. Hecher was supported by the Austrian Science Foundation (Erwin Schrödinger Research Fellowship J0628).

REFERENCES

- Gosling, R. G. and King, D. H. (1975). Ultrasonic angiography. In Marcus, A. W. and Adamson, L. (eds.) *Arteries and Veins*, pp. 61–98. (Edinburgh: Churchill Livingstone)
- Royston, P. (1991). Constructing time-specific reference ranges. *Stat. Med.*, **10**, 675–90
- Yudkin, P. L., Aboualfa, M., Eyre, J. A., Redman, C. W. G. and Wilkinson, A. R. (1987). New birthweight and head circumference centiles for gestational ages 24–42 weeks. *Early Hum. Dev.*, **15**, 45–52
- Kiserud, T., Eik-Nes, S. H., Blaas, H. G. K. and Hellevik, L. R. (1991). Ultrasonographic velocimetry of the fetal ductus venosus. *Lancet*, **338**, 1412–14
- Huisman, T. W. A., Stewart, P. A. and Wladimiroff, J. W. (1992). Ductus venosus blood flow velocity waveforms in the human fetus – a Doppler study. *Ultrasound Med. Biol.*, **18**, 33–7
- Huisman, T. W. A., van den Eijnde, S. M., Stewart, P. A. and Wladimiroff, J. W. (1993). Changes in inferior vena cava blood flow velocity and diameter during breathing movements in the human fetus. *Ultrasound Obstet. Gynecol.*, **3**, 26–30
- Kiserud, T., Eik-Nes, S. H., Hellevik, L. R. and Blaas, H. G. (1992). Ductus venosus – a longitudinal Doppler velocimetric study of the human fetus. *J. Matern. Fetal Invest.*, **2**, 5–11
- Huisman, T. W. A., Stewart, P. A. and Wladimiroff, J. W. (1991). Flow velocity waveforms in the fetal inferior vena cava during the second half of normal pregnancy. *Ultrasound Med. Biol.*, **17**, 679–82
- Huisman, T. W. A., Gittenberger-De Groot, A. C. and Wladimiroff, J. W. (1992). Recognition of a fetal subdiaphragmatic venous vestibulum essential for fetal venous Doppler assessment. *Pediatr. Res.*, **32**, 338–41
- Rizzo, G., Arduini, D., Caforio, L. and Romanini, C. (1992). Effects of sampling sites on inferior vena cava flow velocity waveforms. *J. Matern. Fetal Invest.*, **2**, 153–6
- Kiserud, T., Eik-Nes, S. H., Blaas, H. G. and Hellevik, L. R. (1992). Foramen ovale: an ultrasonographic study of its relation to the inferior vena cava, ductus venosus and hepatic veins. *Ultrasound Obstet. Gynecol.*, **2**, 389–96
- Reed, K. L., Appleton, C. P., Anderson, C. F., Shenker, L. and Sahn, D. J. (1990). Doppler studies of vena cava flows in human fetuses. Insights into normal and abnormal cardiac physiology. *Circulation*, **81**, 498–505
- Rizzo, G., Arduini, D. and Romanini, C. (1992). Inferior vena cava flow velocity waveforms in appropriate- and small-for-gestational-age fetuses. *Am. J. Obstet. Gynecol.*, **166**, 1271–80
- DeVore, G. R. and Horenstein, J. (1993). Ductus venosus index: a method for evaluating right ventricular preload in the second-trimester fetus. *Ultrasound Obstet. Gynecol.*, **3**, 338–42
- Kanzaki, T. and Chiba, Y. (1990). Evaluation of the preload condition of the fetus by inferior vena cava blood flow pattern. *Fetal Diagn. Ther.*, **5**, 168–74
- Kenny, J. F., Plappert, T., Doubilet, P., Saltzman, D. H., Cartier, M., Zollars, L., Leatherman, G. F. and Sutton, M. G. St J. (1986). Changes in intracardiac blood flow velocities and right and left ventricular stroke volumes with gestational age in the normal human fetus: a prospective Doppler echocardiographic study. *Circulation*, **74**, 1208–16
- Reed, K. L., Meijboom, E. J., Sahn, D. J., Scagnelli, S. A., Valdez-Cruz, L. M. and Shenker, L. (1986). Cardiac Doppler flow velocities in human fetuses. *Circulation*, **73**, 41–6
- Reed, K. L., Sahn, D. J., Scagnelli, S., Anderson, C. F. and Shenker, L. (1986). Doppler echocardiographic studies of diastolic function in the human fetal heart: changes during gestation. *J. Am. Coll. Cardiol.*, **8**, 391–5
- van der Mooren, K., Barendregt, L. G. and Wladimiroff, J. W. (1991). Fetal atrioventricular and outflow tract flow velocity waveforms during normal second half of pregnancy. *Am. J. Obstet. Gynecol.*, **165**, 668–74
- Tulzer, G., Khowsathit, P., Gudmundsson, S., Wood, D. C., Tian, Z.-Y., Schmitt, K. and Huhta, J. C. (1994). Diastolic function of the fetal heart during second and third trimester: a prospective longitudinal Doppler-echocardiographic study. *Eur. J. Pediatr.*, **153**, 151–4
- Carceller-Blanchard, A.-M. and Fouron, J.-C. (1993). Determinants of the Doppler flow velocity profile through the mitral valve of the human fetus. *Br. Heart. J.*, **70**, 457–60